Surface-Enhanced Raman Scattering-Based Detection of the Interactions between the Essential Cell Division FtsZ Protein and Bacterial Membrane Elements

Rubén Ahijado-Guzmán,[†] Paulino Gómez-Puertas,[‡] Ramón A. Alvarez-Puebla,[§,#,*] Germán Rivas,[†,#] and Luis M. Liz-Marzán[§,#,*]

[†]Centro de Investigaciones Biológicas, CSIC, c/Ramiro de Maeztu 9, 28040 Madrid, Spain, [‡]Centro de Biología Molecular "Severo Ochoa" (CSIC-UAM), c/Nicolás Cabrera 1, 28049-Madrid, Spain, and [§]Departamento de Química Física, Universidade de Vigo, 36310 Vigo, Spain. [#]These senior authors contributed equally.

ABSTRACT Surface-enhanced Raman scattering (SERS) spectroscopy has been applied to detect the interaction of the FtsZ protein from *Escherichia coli*, an essential component of the bacterial division machinery, with either a soluble variant of the ZipA protein (that provides membrane tethering to FtsZ) or the bacterial membrane (containing the full-length ZipA naturally incorporated), on silver-coated polystyrene micrometer-sized beads. The engineered microbeads were used not only to support the bilayers but also to offer a stable support with a high density of SERS hot spots, allowing the detection of ZipA structural changes linked to the binding of FtsZ. These changes were different upon incubating the coated beads with FtsZ polymers (GTP form) as compared to oligomers (GDP form) and more pronounced when the plasmonic sensors were coated with natural bacterial membranes.

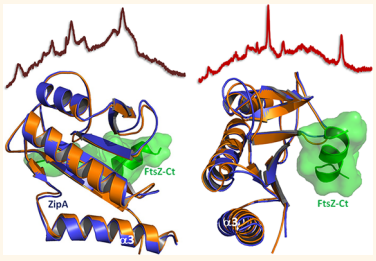

KEYWORDS: bacterial division · FtsZ · label-free sensors · SERS · protein–membrane interactions

The detection of interactions between soluble proteins and membrane receptors at the membrane environment is very important for biological and pharmacological research, as many biochemical processes involve the presence of membranes, and therefore a significant amount of the successful drugs in the market target membrane-associated proteins. The understanding of these processes is key for the development of new families of therapeutic agents, in particular of those targeting protein–membrane receptor interactions.[1,2] The bacterial cell division machinery is a good example of an essential dynamic macromolecular assembly process that takes place at the membrane. The first known event occurring during the bacterial division process is the interaction of the soluble cytoplasmic protein FtsZ with the membrane-bound protein ZipA to form the proto-ring.[3] When FtsZ and ZipA interact, conformational changes occur in the C-terminal domain of ZipA.[4] The understanding of the FtsZ–ZipA interaction within the lipid membrane is of special interest, as it is essential for the bacterial cell division process[5] and, consequently, an important milestone in the development of new families of antibiotics.

Although nanoplasmonics has sufficiently matured to provide suitable tools for studying the mechanisms underlying the interaction between biomacromolecules, proteins in this case, an important factor is still the engineering of a plasmonic surface with sufficient colloidal stability to reproduce the natural conditions involved in biorelated problems. In principle protein–membrane interactions can be measured by fluorescence-based assays using membrane-coated polymer beads. Unfortunately, although this method is extremely sensitive, the low-level structure of fluorescence signals provides limited information about the interaction events. In contrast, surface-enhanced Raman scattering (SERS) spectroscopy[6,7] is an ultrasensitive molecular spectroscopy technique for which detection limits down to the single molecule have been demonstrated.[8] Additionally, SERS is a vibrational spectroscopy, and thus it provides detailed information about the

* Address correspondence to ramon.alvarez@uvigo.es; lmarzan@uvigo.es.

Received for review June 26, 2012 and accepted July 23, 2012.

Published online July 23, 2012
10.1021/nn302825u

structure, conformation, and environment of the given molecular target, and, more importantly, experiments can be carried out under biological conditions.[9] These features make SERS particularly suitable for the characterization of protein or nucleic acid interactions inducing conformational changes.[10−15] However, working with plasmonic nanoparticles and proteins is usually demanding due to either the size of the target analyte as compared with that of the substrate or the need of using solvents with high ionic strength (*i.e.*, PBS or other biological buffers) to avoid protein denaturation. Thus, to properly address this drawback, a considerable effort is required toward the preparation of highly stable while optically active materials, to be used as both supports and optical enhancers. During the last years our group has pioneered the engineering of colloidally stable, optically dense discrete particles comprising a polymeric or inorganic micrometer- or submicrometer-particle core homogeneously coated with the desired plasmonic nanostructure.[16−18] In this work, we have taken advantage of these fabrication protocols to engineer polystyrene microparticles coated with gold and silver (PS@Au@Ag), which display high optical activity, for the immobilization of a bacterial membrane and the study of the structural behavior of membrane proteins during the cell division process.

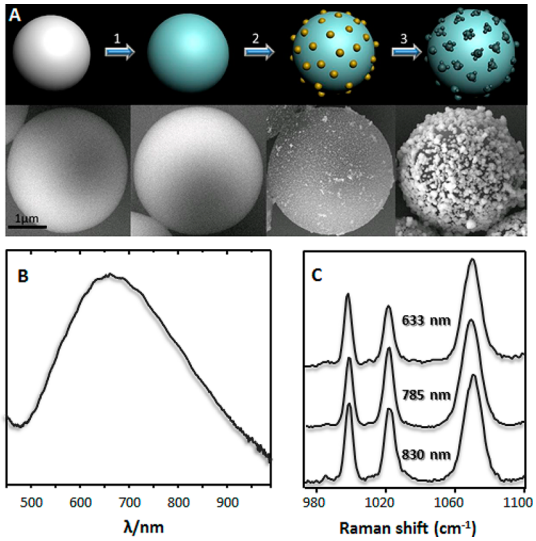

Figure 1. (A) Scheme of the preparation of PS@Au@Ag beads and corresponding SEM characterization. Step 1: Micrometer-sized polystyrene beads were wrapped with polyelectrolytes by sequential LbL self-assembly of PSS, PDDA, PSS, and PAH. Step 2: 15 nm gold nanoparticles were adsorbed onto the functionalized surface of the beads. Step 3: Silver was epitaxially grown on the adsorbed gold nanoparticle surfaces to obtain the final nanocomposite material. (B) vis−NIR spectrum of the PS@Au@Ag beads in water. (C) SERS spectra of benzenethiol on PS@Au@Ag measured upon excitation with 633, 785, and 830 nm laser lines.

RESULTS AND DISCUSSION

PS@Au@Ag microparticles were prepared by using the protocols described in previous reports,[16,19] with slight modifications. A scheme illustrating the different steps involved in the fabrication of the hybrid material, together with their scanning electron microscopy (SEM) characterization, is shown in Figures 1A, S1, and S2. Briefly, the positively charged surface of the selected support, in this case homogeneous polystyrene beads with 3 μm diameter, was sequentially coated with polyelectrolytes of opposite charge, namely, polystyrenesulfonate (PSS, negative), poly(diallyldimethylammonium chloride) (PDDA, positive), again PSS, and finally, poly(allylamine hydrochloride) (PAH, positive), so as to improve the homogeneity of the coating. The outer PAH layer generates a highly positively charged surface (zeta potential +35 mV) that is appropriate for the adsorption of negatively charged gold nanoparticles (zeta potential −40 mV) (step 2). Upon extensive washing to ensure that all nonadsorbed gold nanoparticles were removed, those that remained adsorbed were epitaxially overgrown with silver by *in situ* reduction of Ag^+, using ascorbic acid in a glycine buffer (pH 9.5), at room temperature (step 3). It is interesting to note that gold seeds are preferred over silver for subsequent silver growth, mainly due to their higher chemical stability.[20] After systematic variation of the amount of added Ag^+ between 0.6 and 2.4 μmol per mg of polymer beads, an Ag^+ concentration of 1.8 μmol per mg of beads was selected as optimal, since lower concentrations did not result in suitable interparticle plasmon coupling, while higher concentrations yielded interconnected particles with localized surface plasmon resonance (LSPR) radiative damping.[21] As a final product, this preparation process resulted in micrometer-sized hybrid plasmonic particles with a homogeneous coating of interacting silver particles[19] of *ca.* 50 nm in size.

The optical properties of the material were characterized by vis−NIR spectroscopy from a dispersion of the silver-coated beads, showing a maximum centered at 660 nm (Figure 1B). The optical enhancing properties of the nanostructured microbeads were tested through SERS measurements using benzenethiol (BT) as a model molecular probe. The SERS spectra of BT at different excitation wavelengths were dominated by the vibrational modes of BT corresponding to the ring breathings (999 and 1073 cm^{-1}) and the C−H in-plane bending (1023 cm^{-1}).

We devised several experiments of increasing complexity to study by SERS the FtsZ−ZipA interaction, which is relevant in the initial stages of division in *Escherichia coli*. ZipA is a 328-amino-acid protein that is composed of four domains.[22] However, the binding activity toward FtsZ is localized in the C-terminal domain (residues 189−328). Therefore, mutagenesis of the ZipA gene to produce a soluble variant of the

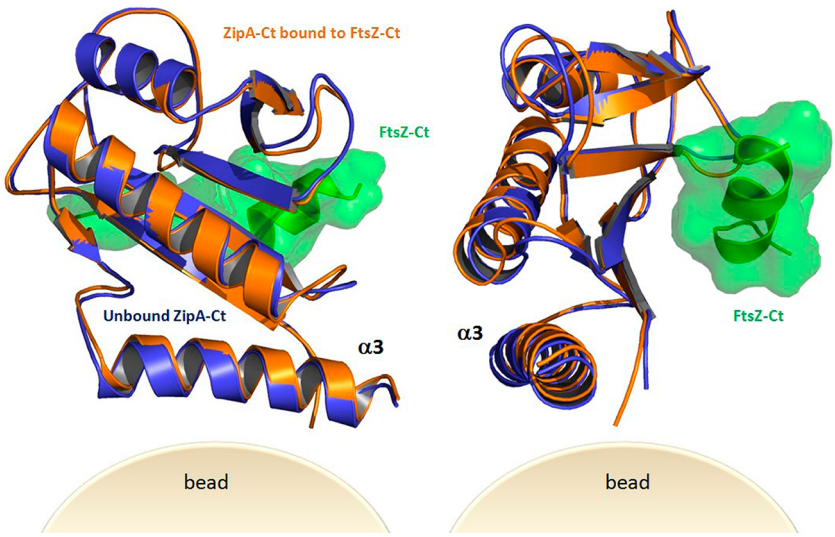

Figure 2. Conformations of sZipA in the absence and in the presence of FtsZ . Spiral: α-helix; arrow: β-sheet; line: random coil. These structures can be accessed free of charge from the Protein Data Bank (access numbers: 1F46A and 1F47B).[4]

protein (sZipA) was carried out by removing the part ranging from the N-terminal domain to the P/Q domain of native ZipA (amino acids 1−188), while preserving the bioactivity[23] and also keeping the hexahistidine tag, which is known to bind strongly to silver and gold.[24] In the case of FtsZ, the wild protein was expressed, extracted, and purified from *E. coli*.[25] Notably, FtsZ has GTPase activity[26] and, *in vitro*, forms a variety of polymers in a GTP-dependent manner.[27−30] Thus, in a first approach sZipA protein was directly attached to PS@Au@Ag beads through the hexahistidine tag, in a buffer solution (50 mM Tris-HCl, pH 7.5, 100 mM KCl, 5 mM $MgCl_2$). It is worth noting that different amounts of sZipA (5 to 20 μM) were added to maximize the SERS signal, which was found to be best for a concentration of 15 μM in dispersions containing 3.3 mg of beads per mL. To investigate the interactions of sZipA with FtsZ, 25 μM FtsZ was added to the PS@Au@Ag-ZipA sample, in the absence or presence of GTP.

As an indication, Figure 2 shows the overlapped conformations of sZipA before and after interaction with FtsZ.[4] On the other hand, Figure 3 shows the SERS spectra for sZipA attached to the beads, with and without FtsZ, in the presence and absence of GTP. The SERS spectrum of sZipA (Figure 3) is dominated by bands that can be assigned to different amino acid residues, for example, 1600 cm^{-1} (Phe, Tyr), 1460 cm^{-1} (Ala, Ile, Val, Leu, Tyr), 1319 cm^{-1} (Ala, Lys, Ile, Val, Ser, Gly, Tyr), 1199 cm^{-1} (Phe, Tyr), 1031 cm^{-1} (Phe, Tyr), 1000 cm^{-1} (Phe), 938 cm^{-1} (Leu, Lys, Val), 848 cm^{-1} (Ile, Tyr), and 785 cm^{-1} (Ala, Trp, Phe).[31−33] All these residues, except Phe, are components of the α3-helix (Figure 2), which is the domain located closer (1.2 nm) to the silver surface. The closest Phe residue is around 1.5 nm away from the surface (in the α2-helix); however the position of its aromatic ring facing down and almost normal to the silver surface notably

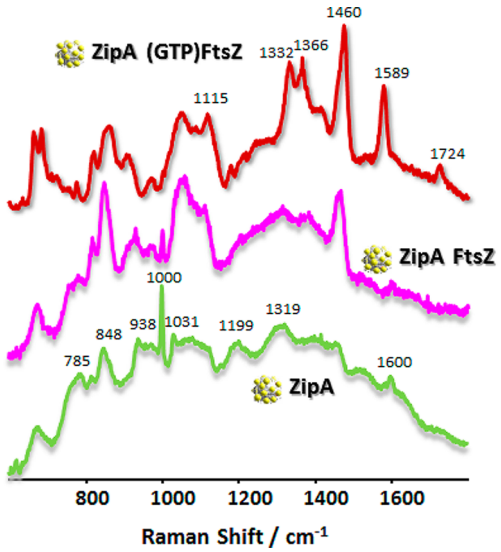

Figure 3. SERS spectra of ZipA on PS@Au@Ag beads, before and after interaction with FtsZ, in the presence and absence of GTP. Samples were illuminated with a 785 nm laser line to avoid damaging the proteins.

increases its signal, in full agreement with surface selection rules.[34]

When FtsZ is added in the presence of GDP (absence of GTP), the protein self-associates in a noncooperative fashion, with the hexamer being the largest oligomeric species present at significant abundance.[23] The SERS spectrum of the complex sZipA−FtsZ oligomer resembles that of the sZipA alone but with subtle differences, especially in the relative intensity of the main bands. FtsZ interacts especially with the β3−6 sheets (Figure 2), which are relatively far away from the surface (*ca.* 3 nm). However, conformational changes in the β-sheets lead to a slight conformational change of the entire sZipA, then promoting a putative change in its orientation on the metallic surface. These small variations

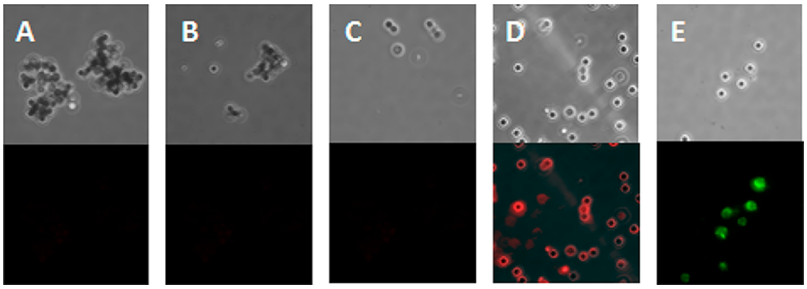

Figure 4. Optical (upper panel) and fluorescence (lower panel) images of plasmonic particles incubated with (A) DiI C18; (B) anti-ZipA + anti-rabbit-488; and (C) anti-rabbit-488. Plasmonic particles coated with the inner membrane incubated with (D) DiI C18 and (E) anti-ZipA + anti-rabbit-488.

resemble those reported by monocrystal X-ray diffraction[4] (Figure 2).

In the presence of GTP, FtsZ assembles into polymer fibrils. Besides the changes seen with the oligomeric FtsZ complex (Figure 3), large enhancements of several bands at 1580 cm^{-1} (Tyr), 1366 and 1332 cm^{-1} (Trp, Val), 1115 cm^{-1} (Ala), and 909 cm^{-1} (Ala) can be observed, indicating a closer proximity of the α3-helix to the silver surfaces. Additionally, new SERS bands appear at 1724 cm^{-1} (amide I) and 1178 cm^{-1} (Tyr). Although the interaction of some of their residues within the plasmonic surface cannot be discarded, due to the size of the FtsZ polymers, the difference of both vibrational spectra of sZipA seems to reveal a different structural conformation of ZipA in the presence of oligomers and polymers.

In subsequent experiments, bacterial membranes were deposited onto the plasmonic beads. The inner membrane vesicles were isolated from wild-type *E. coli* (strain JM600) exponential phase culture.[35] The inner and outer membranes were separated by sucrose gradient centrifugation,[36] washed and diluted to reach 20 absorbance units at 280 nm, and stored frozen.[37] For the deposition, the membranes were added to the bead dispersion and incubated at 37 °C. In this case, ZipA is a natural component of the bacterial membrane. In order to confirm the successful immobilization of the membranes onto the beads, fluorescence images were acquired using DiI C18, which selectively attaches to the lipidic membranes, and anti-ZipA + anti-rabbit-488, which selectively recognizes the ZipA membrane protein. Figure 4 shows that fluorescence is emitted only by the samples coated with the membrane. Control experiments carried out on the bare PS@Au@Ag show no fluorescence, thus evidencing the absence of nonspecific adsorption of the dyes and the successful immobilization of the membrane.

The PS@Au@Ag@inner membrane beads were characterized by SERS prior to the interaction with the FtsZ protein (Figure 5). The SERS spectrum is dominated by the lipidic CH_2 scissoring and twisting (1378 and 1322 cm^{-1}) and the alkyl skeletal vibrations (1125 and 1033 cm^{-1}).[38] Concerning the polar headgroups,

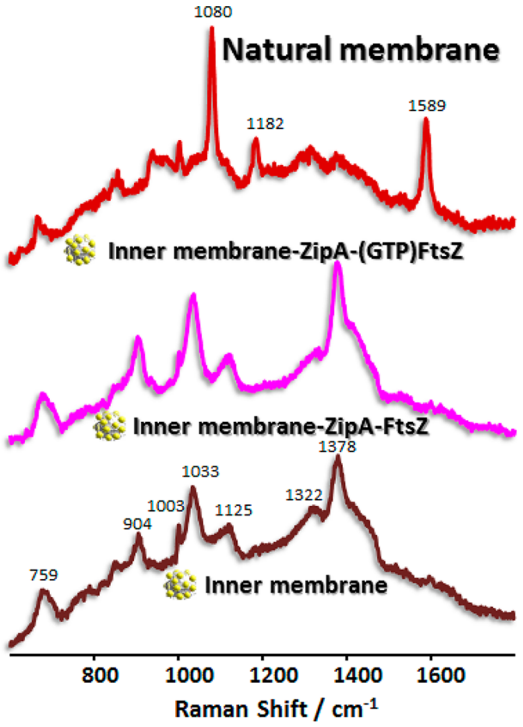

Figure 5. SERS spectra of the PS@Au@Ag@inner membrane-ZipA before and after the interaction with FtsZ, in the presence and absence of GTP.

the SERS bands corresponding to the C−N stretching of the O−C−C−N+ segment are observed at 1003 cm^{-1}, while 904 and 759 cm^{-1} are ascribed to the trans conformation of this fragment as described previously.[39] Notably, several amino acids can be recognized as well, especially those of Phe (1000 cm^{-1}) and Tyr (1319 cm^{-1}), which is consistent with the high SERS cross sections of their aromatic groups, as compared with the essentially alkylic nature of the membrane. Minimum changes can be inferred from the spectrum when the FtsZ oligomers (GDP forms) are added as compared with those detected in the previous experiment. However, in the presence of FtsZ polymers (GTP form) the SERS spectrum shows notable differences as compared to that of the membrane. Basically, the spectrum presents several new bands at 1589 cm^{-1} (Phe, Tyr), 1182 cm^{-1} (Tyr, Phe,

C−C stretch), and 1080 cm^{-1} (C−C skeleton gauche structure). On the other hand, bands at 1380 cm^{-1} (CH_2 scissoring from lipid chains) and 906 cm^{-1} (C−C stretch and skeletal bend) decrease in intensity. The presence of these amino acid bands, together with the shifts in those of the membrane, suggests that the interaction of FtsZ polymers with ZipA induces structural changes not only in this anchoring protein but also in other membrane elements. This can be due to the association of several ZipA molecules at the membrane, establishing additional contacts with FtsZ elements.

CONCLUSIONS

The vibrational changes in SERS spectra of either the soluble variant of ZipA or the bacterial inner membrane (with ZipA naturally incorporated) on silver-coated microbeads are different in the presence of FtsZ polymers (GTP forms) as compared with GTP-free ZipA or ZipA with FtsZ oligomers (GDP forms), these spectral changes being more pronounced in the case of the membrane-coated particles. This system provides the benefits of the very high sensitivity of SERS spectroscopy to detect small structural changes of membrane-associated receptors (the ZipA protein) upon binding of soluble macromolecules (FtsZ polymers) that interact with moderate affinity. These plasmonic sensors can be exploited to develop ultrafast assays to screen for substances that interfere with the attachment of FtsZ to the membrane, with potential antimicrobial activity.

EXPERIMENTAL SECTION

Materials. Reagents, metallic salts, buffers, microsized polystyrene (PS) beads (3 μm), guanosine 5′-diphosphate (GDP), guanosine 5′-triphosphate (GTP), benzenethiol (BT), and other analytical grade chemicals were acquired from Sigma-Aldrich or Merck. All proteins were extensively dialyzed against the working buffer, 50 mM Tris-HCl pH 7.5, 100 mM KCl, 5 mM $MgCl_2$.

Polystyrene Microbeads Functionalization and Coating. Polystyrene microbeads of 3 μm diameter (0.5 mL of a 100 mg mL^{-1} suspension) were first wrapped with alternating polyelectrolyte monolayers using the layer-by-layer (LbL) electrostatic self-assembly protocol.[40] Four alternate layers were deposited: polystyrenesulfonate (M_w = 1 000 000), poly(diallyldimethylammonium chloride) (M_w = 100 000−200 000), PSS, and, finally, poly(allylamine hydrochloride) (M_w = 56 000). Polystyrene microbeads (0.5 mL of a 100 mg mL^{-1} suspension) were added to 25 mL of a 2 mg mL^{-1} PSS aqueous solution containing 0.5 M NaCl. After 30 min of sonication and 2 h of agitation the PS microbeads were extensively washed with Milli-Q water and centrifuged (5000 rpm, 15 min). The same protocol (concentrations, elapsed times, and washing protocol) was carried out for depositing subsequent layers of PDDA, PSS, and PAH polyelectrolytes. Gold seeds (15 nm) were prepared by heating 50 mL of 0.5 mM $HAuCl_4$ to boiling and adding 2.5 mL of 1% sodium citrate solution under mechanical stirring.

The adsorption of the particles onto the functionalized PS beads was carried out by adding 12 mL of as-prepared 0.5 mM seeds to 4 mL of PS beads (5 mg mL^{-1}). After 15 min of sonication, the PS@Au beads were washed first three times by centrifugation (3000 rpm, 15 min) and then three times by decantation with Milli-Q water. Silver was grown on gold seeds as follows: 4 mL of PS@Au 5 mg mL^{-1} was mixed with a solution containing 33 mL of 0.4 M glycine at pH 9.5 and 2.4 mL of 15 mM Ag_2SO_4.[16] During sonication in cold water, 3.3 mL of 0.1 M ascorbic acid was added. After 1 h in a sonication bath, the solution was washed with Milli-Q water three times by centrifugation (3000 rpm, 15 min) and three times by decantation.

Protein Purification. *Escherichia coli* wild-type FtsZ was expressed and purified by the calcium-induced precipitation method.[25] FtsZ was frozen and stored at −80 °C in 20 μL aliquots. In this study FtsZ was used in different bound states: GDP-FtsZ (nonpolymerized protein) and GTP-FtsZ (polymerized protein).

Mutagenesis of the ZipA gene, overexpression, and purification were carried out by removal from the N-terminal domain to the P/Q-domain of native ZipA (aminoacids 1−188).[23] The protein preserves the hexahistidine tag. All proteins were extensively dialyzed against 50 mM Tris-HCl pH 7.5, 100 mM KCl, and 5 mM $MgCl_2$.

Isolation of *E. coli* Inner Membranes. The inner membrane vesicles were isolated from wild-type *E. coli* (strain JM600) exponential phase culture.[35] The inner and outer membranes were separated by sucrose gradient centrifugation,[36] washed and diluted to reach 20 absorbance units at 280 nm, and stored frozen at −80 °C.[37]

ZipA Immobilization on the PA@Au@Ag Beads and FtsZ Interaction. PS@Au@Ag beads were washed three times by centrifugation (3000 rpm × 15 min) with 50 mM Tris-HCl pH 7.5, 100 mM KCl, and 5 mM $MgCl_2$. ZipA was equilibrated against the same buffer solution. Different amounts of protein solution were mixed with PS@Au@Ag beads (3.3 mg mL^{-1}) to a final concentration of protein between 5 and 20 μM, and the solution was stored in a soft shaker at 4 °C for 1 h and washed three times (3000 rpm × 15 min) at 4 °C. Finally we found 15 μM to be the optimal concentration of ZipA protein in order to obtain the better SERS signal. The hexahistidine tag from ZipA is strongly attached to the nanostructured silver.[24]

A dispersion of PS@Au@Ag-ZipA beads as described above was mixed with GDP-FtsZ protein and incubated in a soft shaker at 4 °C for 30 min. GDP-FtsZ was previously equilibrated against the working buffer. The final concentrations of beads are 3.3 mg mL^{-1} and FtsZ 25 μM. In the case of GTP-FtsZ, an aliquot of PS@Au@Ag-ZipA-GDP-FtsZ beads described previously was mixed with GTP to a final concentration of 1 mM supplemented with enzymatic GTP-regenerating system, as previously described,[30] and incubated at room temperature for 5 min. The GTP control of soluble PS@Au@Ag-ZipA beads was done without FtsZ.

PS@Au@Ag beads were washed with buffer three times by centrifugation (3000 rpm, 15 min). An aliquot of inner membrane was mixed with washed PS@Au@Ag beads, incubated in a soft shaker for 2 h, and sonicated for 30 s in a 4 °C water bath. Inner membrane coated PS@Au@Ag beads were washed three times (3000 rpm, 15 min), sonicated in a cold water bath for 30 s, and washed three more times. The coated beads were mixed with equilibrated GDP-FtsZ protein and incubated in a soft shaker for 30 min. The final concentration of beads was 3.3 mg mL^{-1} with 25 μM FtsZ. In the case of GTP-FtsZ, an aliquot of GDP-FtsZ-inner-membrane-coated PS@Au@Ag beads was mixed with 1 mM GTP supplemented with enzymatic GTP-regenerating system and incubated at room temperature for 5 min. The GTP control of inner membrane coated PS@Au@Ag beads was done without FtsZ.

Characterization. UV−vis−NIR spectra were recorded using an Agilent 8453 diode array spectrophotometer. Scanning electron microscopy images were obtained with a JEOL JSM6700F microscope operating at an acceleration voltage of 10 kW, and a secondary electron detector mode was used for characterization.

Surface-Enhanced Raman Scattering Spectroscopy. SERS experiments were conducted in a micro-Renishaw InVia Reflex system. The spectrograph uses high-resolution grating (1200 grooves mm^{-1}) with additional band-pass filter optics, a confocal microscope, and a 2D-CCD camera. Excitation was carried out at 785 nm (diode). Measurements were made in a confocal microscope in backscattering geometry using a 100× objective with a NA value of 0.9, providing a spatial resolution of 500 nm with accumulation times of 10 s. For SERS characterization of the PS@Au@Ag beads, 10 μL of a BT solution (10^{-3} M) was added to 1 mL of the sample, reaching a final concentration of 10^{-5} M in BT. A 10 μL amount of the mixture was then cast and air-dried onto a clean glass slide. For SERS measurements 10 μL of the different samples of coated PS@Au@Ag beads was deposited on a clean glass slide. Each sample was prepared at least twice at the same conditions, and at least 10 different beads were measured for each sample to ensure reproducibility.

Conflict of Interest: The authors declare no competing financial interest.

Acknowledgment. We thank Begoña Monterroso (CIB-CSIC) for critical comments and help with microbead assays and Miguel Vicente (CNB-CSIC) for his comments, advice, and support. This work was funded by the European Research Council through Advanced Grant 267867, PLASMAQUO (to L.M.L.-M.), the Human Frontier Science Program through Grant RGP0050/2010 (to G.R.), The European Commission through Contract HEALTH-F3-2009-223431 (to both P.G.P. and G.R.), and the Spanish Government through Grants CTQ2011-23167 (to R.A. A.-P.), BIO2011-28941-C03 (to G.R.), IPT-2011-0964-900000, and SAF2011-13156-E (to P.G.P.). R.A.G. is a JAE-CSIC predoctoral fellow.

Supporting Information Available: TEM and SEM images of SiO_2@Au and SiO_2@Au@Ag particles. This material is available free of charge *via* the Internet at http://pubs.acs.org.

REFERENCES AND NOTES

1. Drews, J. Drug Discovery: A Historical Perspective. *Science* **2000**, *287*, 1960–1964.
2. Galush, W. J.; Shelby, S. A.; Mulvihill, M. J.; Tao, A.; Yang, P.; Groves, J. T. A Nanocube Plasmonic Sensor for Molecular Binding on Membrane Surfaces. *Nano Lett.* **2009**, *9*, 2077–2082.
3. Vicente, M.; Rico, A. I.; Martínez-Arteaga, R.; Mingorance, J. Septum Enlightenment: Assembly of Bacterial Division Proteins. *J. Bacteriol.* **2006**, *188*, 19–27.
4. Mosyak, L.; Zhang, Y.; Glasfeld, E.; Haney, S.; Stahl, M.; Seehra, J.; Somers, W. S. The Bacterial Cell-Division Protein ZipA and its Interaction with an FtsZ Fragment Revealed by X-ray Crystallography. The Protein Data Bank (PDB ID: 1F46). *EMBO J.* **2000**, *19*, 3179–3191.
5. Hale, C. A.; de Boer, P. A. J. Recruitment of ZipA to the Septal Ring of *Escherichia coli* Is Dependent on FtsZ and Independent of FtsA. *J. Bacteriol.* **1999**, *181*, 167–176.
6. Willets, K. A.; Van Duyne, R. P. Localized Surface Plasmon Resonance Spectroscopy and Sensing. *Annu. Rev. Phys. Chem.* **2007**, *58*, 267–97.
7. Moskovits, M. Surface-Enhanced Raman Spectroscopy: a Brief Retrospective. *J. Raman Spectrosc.* **2005**, *36*, 485–496.
8. Kneipp, K.; Wang, Y.; Kneipp, H.; Perelman, L. T.; Itzkan, I.; Dasari, R.; Feld, M. S. Single Molecule Detection Using Surface-Enhanced Raman Scattering (SERS). *Phys. Rev. Lett.* **1997**, *78*, 1667–1670.
9. Alvarez-Puebla, R. A.; Liz-Marzan, L. M. SERS-Based Diagnosis and Biodetection. *Small* **2010**, *6*, 604–610.
10. Cotton, T. M.; Kim, J.-H.; Chumanov, G. D. Application of Surface-Enhanced Raman Spectroscopy to Biological Systems. *J. Raman Spectrosc.* **1991**, *22*, 729–742.
11. Mahmoudi, M.; Lynch, I.; Ejtehadi, M. R.; Monopoli, M. P.; Bombelli, F. B.; Laurent, S. Protein−Nanoparticle Interactions: Opportunities and Challenges. *Chem. Rev.* **2011**, *111*, 5610–5637.
12. Rosi, N. L.; Mirkin, C. A. Nanostructures in Biodiagnostics. *Chem. Rev.* **2005**, *105*, 1547–1562.
13. Sanles-Sobrido, M.; Rodriguez-Lorenzo, L.; Lorenzo-Abalde, S.; Gonzalez-Fernandez, A.; Correa-Duarte, M. A.; Alvarez-Puebla, R. A.; Liz-Marzan, L. M. Label-Free SERS Detection of Relevant Bioanalytes on Silver-Coated Carbon Nanotubes: The Case of Cocaine. *Nanoscale* **2009**, *1*, 153–158.
14. Fabris, L.; Dante, M.; Braun, G.; Lee, S. J.; Reich, N. O.; Moskovits, M.; Nguyen, T. Q.; Bazan, G. C. A Heterogeneous PNA-Dased SERS Method for DNA Detection. *J. Am. Chem. Soc.* **2007**, *129*, 6086–7.
15. Alvarez-Puebla, R. A.; Agarwal, A.; Manna, P.; Khanal, B. P.; Aldeanueva-Potel, P.; Carbo-Argibay, E.; Pazos-Perez, N.; Vigderman, L.; Zubarev, E. R.; Kotov, N. A.; *et al*. Gold Nanorods 3D-Supercrystals as Surface Enhanced Raman Scattering Spectroscopy Substrates for the Rapid Detection of Scrambled Prions. *Proc. Natl. Acad. Sci. U. S. A.* **2011**, *108*, 8157–8161.
16. Tsoutsi, D.; Montenegro, J. M.; Dommershausen, F.; Koert, U.; Liz-Marzan, L. M.; Parak, W. J.; Alvarez-Puebla, R. A. Quantitative Surface-Enhanced Raman Scattering Ultradetection of Atomic Inorganic Ions: The Case of Chloride. *ACS Nano* **2011**, *5*, 7539–7546.
17. Spuch-Calvar, M.; Rodriguez-Lorenzo, L.; Morales, M. P.; Alvarez-Puebla, R. A.; Liz-Marzan, L. M. Bifunctional Nanocomposites with Long-Term Stability as SERS Optical Accumulators for Ultrasensitive Analysis. *J. Phys. Chem. C* **2009**, *113*, 3373–3377.
18. Alvarez-Puebla, R. A.; Liz-Marzan, L. M. Traps and Cages for Universal SERS Detection. *Chem. Soc. Rev.* **2012**, *41*, 43–51.
19. Abalde-Cela, S.; Hermida-Ramon, J. M.; Contreras-Carballada, P.; De Cola, L.; Guerrero-Martinez, A.; Alvarez-Puebla, R. A.; Liz-Marzan, L. M. SERS Chiral Recognition and Quantification of Enantiomers through Cyclodextrin Supramolecular Complexation. *ChemPhysChem* **2011**, *12*, 1529–1535.
20. Rodriguez-Gonzalez, B.; Burrows, A.; Watanabe, M.; Kiely, C. J.; Liz Marzan, L. M. Multishell Bimetallic AuAg Nanoparticles: Synthesis, Structure and Optical Properties. *J. Mater. Chem.* **2005**, *15*, 1755–1759.
21. Schlegel, V. L.; Cotton, T. M. Silver-Island Films as Substrates for Enhanced Raman Scattering: Effect of Deposition Rate on Intensity. *Anal. Chem.* **1991**, *63*, 241–247.
22. Hale, C. A.; de Boer, P. A. J. Direct Binding of FtsZ to ZipA, an Essential Component of the Septal Ring Structure That Mediates Cell Division in *E. coli*. *Cell* **1997**, *88*, 175–185.
23. Martos, A.; Alfonso, C.; Lopez-Navajas, P.; Ahijado-Guzmán, R.; Mingorance, J.; Minton, A. P.; Rivas, G. N. Characterization of Self-Association and Heteroassociation of Bacterial Cell Division Proteins FtsZ and ZipA in Solution by Composition Gradient−Static Light Scattering. *Biochemistry* **2010**, *49*, 10780–10787.
24. Daniel, M.-C.; Astruc, D. Gold Nanoparticles: Assembly, Supramolecular Chemistry, Quantum-Size-Related Properties, and Applications toward Biology, Catalysis, and Nanotechnology. *Chem. Rev.* **2004**, *104*, 293–346.
25. Rivas, G.; Lopez, A.; Mingorance, J.; Minton, A. P.; Ferrándiz, M. J.; Vicente, M.; Zorrilla, S.; Andreu, J. M. Magnesium-Induced Linear Self-Association of the FtsZ Bacterial Cell Division Protein Monomer. The Primary Steps of FtsZ Assembly. *J. Biol. Chem.* **2000**, *275*, 11740–11749.
26. Erickson, H. P.; Taylor, D. W.; Taylor, K. A.; Bramhill, D. Bacterial Cell Division Protein FtsZ Assembles into Protofilament Sheets and Minirings, Structural Homologs of Tubulin Polymers. *Proc. Natl. Acad. Sci. U. S. A.* **1996**, *93*, 519–523.
27. González, J. M.; Vélez, M.; Jiménez, M.; Alfonso, C.; Schuck, P.; Mingorance, J.; Vicente, M.; Minton, A. P.; Rivas, G. Cooperative Behavior of Escherichia coli Cell-Division Protein FtsZ Assembly Involves the Preferential Cyclization of Long Single-Stranded Fibrils. *Proc. Natl. Acad. Sci. U. S. A.* **2005**, *102*, 1895–1900.
28. Mukherjee, A.; Dai, K.; Lutkenhaus, J. Escherichia Coli Cell Division Protein FtsZ is a Guanine Nucleotide Binding Protein. *Proc. Natl. Acad. Sci. U. S. A.* **1993**, *90*, 1053–1057.

29. Anderson, D. E.; Gueiros-Filho, F. J.; Erickson, H. P. Assembly Dynamics of FtsZ Rings in *Bacillus subtilis* and *Escherichia coli* and Effects of FtsZ-Regulating Proteins. *J. Bacteriol.* **2004**, *186*, 5775–5781.
30. González, J. M.; Jiménez, M.; Vélez, M.; Mingorance, J.; Andreu, J. M.; Vicente, M.; Rivas, G. Essential Cell Division Protein FtsZ Assembles into One Monomer-Thick Ribbons under Conditions Resembling the Crowded Intracellular Environment. *J. Biol. Chem.* **2003**, *278*, 37664–37671.
31. Tuma, R. Raman Spectroscopy of Proteins: From Peptides to Large Assemblies. *J. Raman Spectrosc.* **2005**, *36*, 307–319.
32. Thomas, G. J. New Structural Insights from Raman Spectroscopy of Proteins and Their Assemblies. *Biopolymers* **2002**, *67*, 214–225.
33. Overman, S. A.; Thomas, G. J. Raman Markers of Nonaromatic Side Chains in an α-Helix Assembly: Ala, Asp, Glu, Gly, Ile, Leu, Lys, Ser, and Val Residues of Phage fd Subunits. *Biochemistry* **1999**, *38*, 4018–4027.
34. Moskovits, M.; Dilella, D. P.; Maynard, K. J. Surface Raman-Spectroscopy of a Number of Cyclic Aromatic-Molecules Adsorbed on Silver - Selection-Rules and Molecular-Reorientation. *Langmuir* **1988**, *4*, 67–76.
35. Rueda, S.; Vicente, M.; Mingorance, J. Concentration and Assembly of the Division Ring Proteins FtsZ, FtsA, and ZipA during the *Escherichia coli* Cell Cycle. *J. Bacteriol.* **2003**, *185*, 3344–3351.
36. Osborn, M. J.; Gander, J. E.; Parisi, E.; Carson, J. Mechanism of Assembly of the Outer Membrane of *Salmonella typhimurium*. *J. Biol. Chem.* **1972**, *247*, 3962–3972.
37. Jiménez, M.; Martos, A.; Vicente, M.; Rivas, G. Reconstitution and Organization of Escherichia coli Proto-ring Elements (FtsZ and FtsA) inside Giant Unilamellar Vesicles Obtained from Bacterial Inner Membranes. *J. Biol. Chem.* **2011**, *286*, 11236–11241.
38. Lhert, F.; Capelle, F.; Blaudez, D.; Heywang, C.; Turlet, J. M. Raman Spectroscopy of Phospholipid Black Films. *J. Phys. Chem. B* **2000**, *104*, 11704–11707.
39. Clark, R. J. H.; Hester, R. E. *Advances in Infrared and Raman Spectroscopy*; Wiley: New York, 1984.
40. Decher, G. Fuzzy Nanoassemblies: Toward Layered Polymeric Multicomposites. *Science* **1997**, *277*, 1232–1237.